

1. SPH model

To understand the formation of the Hobson family, we computed SPH models of single as well as binary asteroid breakups. Binarity is important, because the initial shock wave cannot propagate to the secondary, but its mass contributes to the total gravity (Rožehnal et al. 2016). Moreover, it can potentially explain the size-frequency distribution (SFD), which contains two similarly-sized bodies.

We used the `OpenSPH` code (Ševeček et al. 2019; Ševeček 2019) for all SPH and N-body simulations. There are substantial improvements with respect to our previous work (Ševeček et al. 2017). In particular, (i) we include self-gravity already in the fragmentation phase; (ii) this allows us to prolong it up to 1000 s, until fragments are separated; (iii) the primary and the secondary (if present) rotate synchronously; (iv) we do not assume perfect merging in the reaccumulation phase to avoid super-critical rotators; (v) we suppress merging efficiency to create similar spatial structures as in full SPH runs; (vi) we account for stochasticity by performing several simulations with almost the same initial conditions. The setup is described in detail in Sec. A.

After trial-and-error, we found two solutions for the SFD: either a single asteroid breakup which results in a similarly-sized pair, or a binary asteroid, with a breakup of the primary and the secondary preserved as a pair component.

In the case of a single asteroid, we assumed the target radius $R_1 = 5$ km, the impactor radius $R_i = 0.8$ km, the impact angle $\phi = 30^\circ$, and the impact velocity $v = 5$ km s⁻¹. The resulting SFD is shown in Fig. 1 (top). It is a good match, although it is still slightly 'overshoot', with a pair of 3.0 km fragments. They are not bound. A sequence of plots showing the spatial distribution of SPH particles (Fig. 2, top) demonstrates it is an head-on impact, which splits the target approximately in two halves, moving away from each other, which eventually reaccumulate and form the pair (Fig. 2, bottom). Obtaining this kind of SFD, requires some fine-tuning of impact parameters and multiple simulations at the same time, because transient pairs often merge. Let us also point out there is a lot of 'waste' (a.k.a. non-reaccumulated fragments) because the reaccumulation is no longer idealized.

For a binary, we assumed the following parameters: the primary radius $R_1 = 3.75$ km, secondary radius $R_2 = 1.25$ km, impactor radius $R_i = 0.7$ km, spin rate(s) $\omega = 2.79383$ rev. d⁻¹, impact angle $\phi = 60^\circ$, impact velocity $v = 5$ km s⁻¹, binary separation $r = 10$ km, and orbital velocity $v_k = 0.0020317$ km s⁻¹. The SFD is shown in Fig. 1 (bottom). This time we performed 10 simulation with almost the same initial conditions ($v = 4.96$ to 5 km s⁻¹ $\phi = 60$ to 60.5°). It is then clear the process is stochastic. The primary was damaged, fragmented and dispersed similarly as before, and usually reaccreted 'elsewhere' as a single 3-km-sized body (see Fig. 3). Consequently, the former binary was unbound. We often obtained a pair though, because the secondary is always preserved. In the process, it is only marginally damaged at surface by low-speed secondary impacts, but its interior never experienced heating. This is a major advantage of the binary model, because it consistently produces similarly-sized pairs.

References

- Diehl, S., Rockefeller, G., Fryer, C. L., Riethmiller, D., & Statler, T. S. 2012, arXiv e-prints, arXiv:1211.0525
- Rožehnal, J., Brož, M., Nesvorný, D., et al. 2016, MNRAS, 462, 2319
- Ševeček, P. 2019, OpenSPH: Astrophysical SPH and N-body simulations and interactive visualization tools
- Ševeček, P., Brož, M., Nesvorný, D., et al. 2017, Icarus, 296, 239

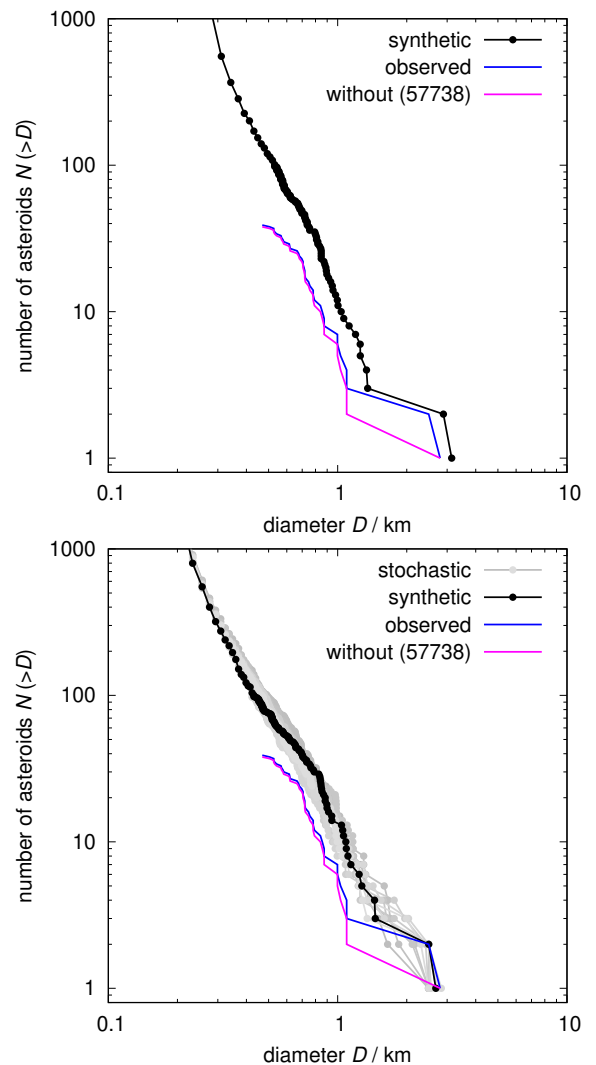


Fig. 1. Cumulative size-frequency distributions $N(>D)$ of fragments for a collision with a single asteroid (top), and with a wide binary (bottom). The synthetic SFD (black) is compared with other similar simulations (gray) and the observed SFD of the Hobson family (blue), possibly without the second largest body (magenta). Both models can produce two similarly-sized large fragments.

- Tillotson, J. H. 1962, Metallic Equations of State For Hypervelocity Impact, General Atomic Report GA-3216. 1962. Technical Report
- Ševeček, P., Brož, M., & Jutzi, M. 2019, A&A, 629, A122

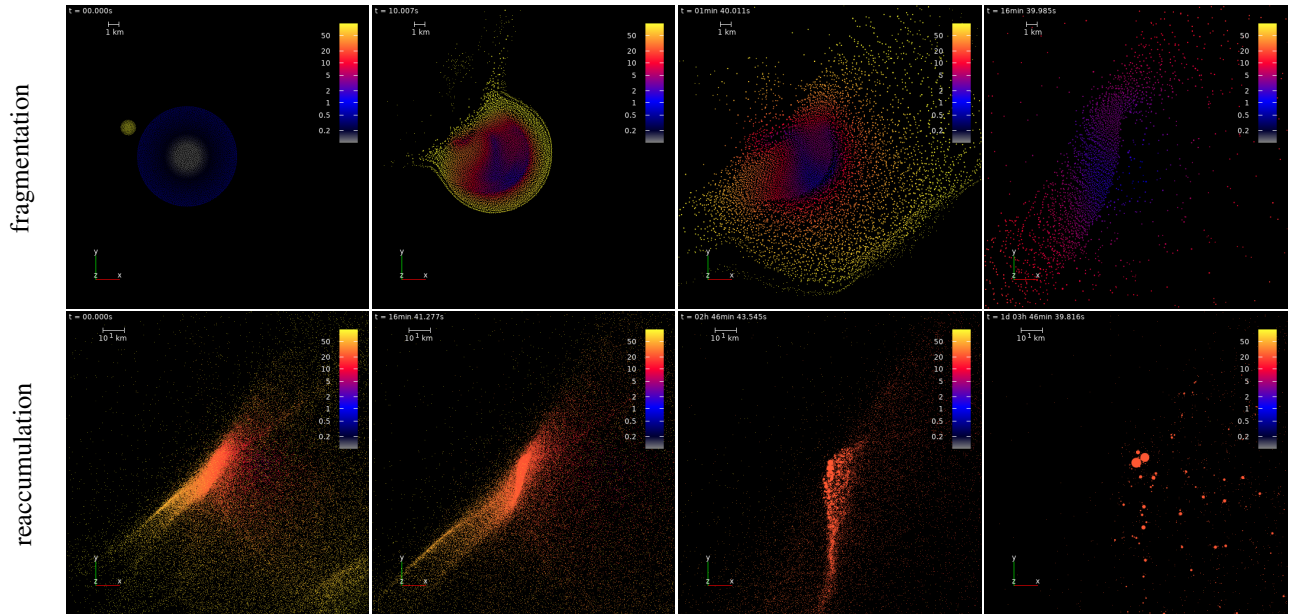


Fig. 2. Simulation of a single asteroid breakup. The basic parameters were: the target radius $R_1 = 5$ km, the impactor radius $R_i = 0.8$ km, the impact velocity $v = 5$ km s $^{-1}$, and the impact angle $\phi = 30^\circ$ (head-on). The fragmentation phase is shown for the times $t = 0, 10, 100, 10^3$ s (top), and the reaccumulation phase for $t = 0, 10^3, 10^4, 10^5$ s (after handoff; bottom). The spatial distribution of SPH particles is plotted only within a limited range of the coordinate $z \in (-1, 1)$ km to clearly see the interiors of bodies. Colours correspond to the velocity v . Individual panels can be described as follows: (a) the initial conditions, (b) high-speed ejecta, (c) formation of a cavity with low relative speeds, (d) 'splitting' of the target, (e) handoff, (f) streams of high-speed particles, (g) ongoing reaccumulation, (h) formation of an unbound pair.

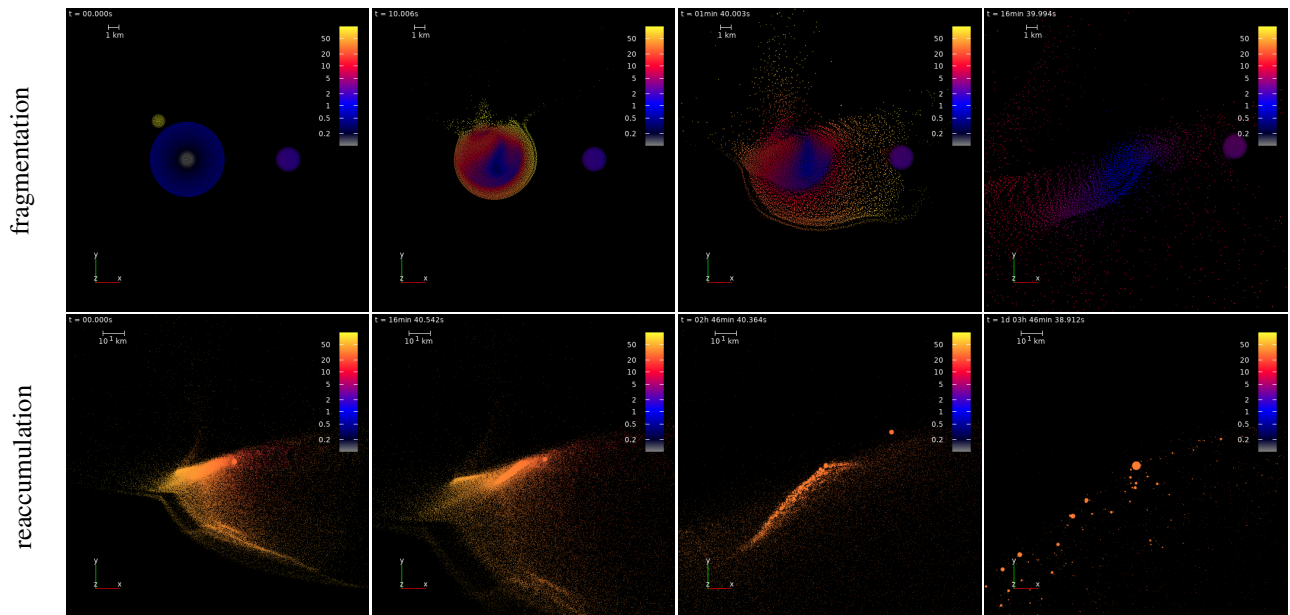


Fig. 3. Same as Figure 2 for a wide binary. The basic parameters were: the primary radius $R_1 = 3.75$ km, the secondary radius $R_2 = 1.25$ km, $R_i = 0.7$ km, $v = 5$ km s $^{-1}$, and $\phi = 60^\circ$ (oblique). Individual panels can be alternatively described as follows: (a) orbital motion of the binary, (b) ejecta also from the primary surface, (c) secondary impacts onto the secondary, (d) not splitting of the primary, (e) handoff with the preserved secondary, (f) onset of reaccumulation of other fragments, (g) the escaping secondary, (h) the reaccumulated primary and the secondary (not shown), which together form a distant pair.

Appendix A: Setup of SPH simulations

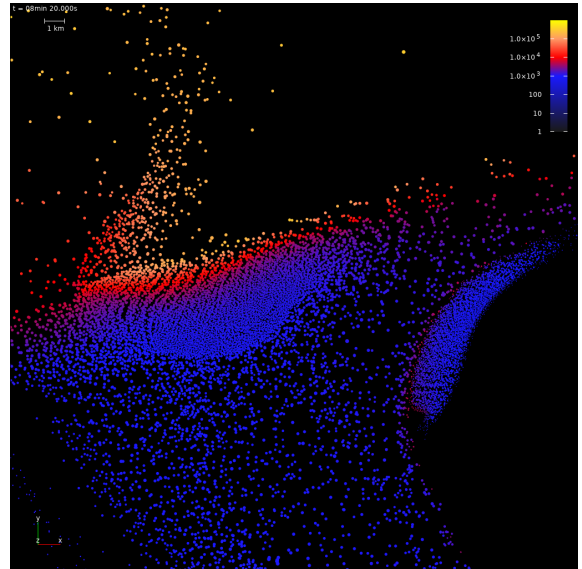


Fig. A.1. Simulation of a contact binary breakup. The spatial distribution of SPH particles is shown within a limited range of $z \in (-1, 1)$ km and for $t = 500$ s. Colours correspond to the internal energy U . The primary was dispersed after a collision with the impactor (not shown). The secondary (on the right) was ‘squeezed’ due to a low-speed collision with the primary.

All materials were similar to monolithic basalt, with the density $\rho = 2700 \text{ kg m}^{-3}$, the bulk modulus $B = 2.67 \cdot 10^{10} \text{ Pa}$, the shear modulus $\mu = 2.27 \cdot 10^{10} \text{ Pa}$, the elastic modulus $\epsilon = 8 \cdot 10^9$, Tillotson (1962) equation of state parameters $a = 0.5$, $b = 1.5$, B as above, $\alpha = 5$, $\beta = 5$, incipient vaporisation energy $U_{iv} = 4.72 \cdot 10^6 \text{ J}$, complete vaporisation energy $U_{cv} = 1.82 \cdot 10^7 \text{ J}$, sublimation energy $U_{sub} = 4.87 \cdot 10^8 \text{ J}$, initial scalar damage $D = 0$, von Mises rheology, von Mises limit $Y = 3.5 \cdot 10^9 \text{ Pa}$, melting energy $U_{melt} = 3.4 \cdot 10^6 \text{ J}$, Weibull coefficient $k = 4 \cdot 10^{35}$, Weibull exponent $m = 9$. We also performed tests with the Drucker–Prager rheology, but if pressure-dependent limit $Y(P)$ for a peak pressure P is similar to Y above, the outcome is similar. We do not analyse shapes of individual fragments.

The fragmentation phase duration was 10^3 s. The time step was controlled by the Courant number $C = 0.2$, the derivative factor 0.2, and the divergence factor 0.005. We used the asymmetric SPH solver, the standard SPH discretisation, the correction tensor for rotation, the predictor–corrector integrator, we summed over undamaged particles. The artificial viscosity parameters were $\alpha = 1.5$, $\beta = 3$. We also used the Barnes–Hut gravity solver, with the opening angle $\phi = 0.5$, the multipole order $\ell = 3$, and eventually an equal-volume handoff.

The reaccumulation phase duration was 10^5 s, computed with the leap-frog integrator, a ‘merge-or-bounce’ collisional handler, and a ‘repel-or-merge’ overlap handler. The derivative factor was 0.005. For the normal restitution we assumed a value 0.5, the tangential restitution 1, the merge velocity limit $\alpha_v = 0.25$, where the condition for merging is:

$$v_{\text{rel}} < \alpha_v \sqrt{\frac{2G(m_1 + m_2)}{r_1 + r_2}}; \quad (\text{A.1})$$

The simulations presented in Sec. 1 were performed with the following numerical setup and material parameters (see also Ševeček 2019 for details). The number of particles was $N = 10^5$, 10^4 , and 10^3 for the primary, the secondary, and the impactor. We used Diehl et al. (2012) random-yet-isotropic distribution of particles.

the merge rotation limit $\alpha_\omega = 1.0$. The final SFD is computed from masses. The model is still somewhat resolution dependent, because the number of particles determines the smallest ‘block’ size, and the SFD is built from these blocks.

Appendix B: Contact binary

We also tested an impact to a contact (or close) binary, which is a different regime. The secondary was slowly pushed by the primary and 'squeezed' along the perpendicular direction (see Fig. A.1). All these motions were highly subsonic. Eventually, most of its mass was reaccreted, because mutual velocities are relatively low compared to direct ejecta from the primary. The reaccreted secondary must have a different internal structure, with damaged material and fresh surface. This is different from the case of a wide binary, discussed in the main text. Consequently, contact binaries seem to be 'ideal' systems, where materials are subjected to both supersonic/subsonic processes, high/low pressure, etc.